A multiphoton objective design with incorporated beam splitter for enhanced fluorescence collection

Jesse D. McMullen[1] and Warren R. Zipfel[1,2*]

[1]*School of Applied and Engineering Physics, Cornell University, Ithaca, New York 14853, USA*
[2]*Department of Biomedical Engineering, Cornell University, Ithaca, New York 14853, USA*
**wrz2@cornell.edu*

Abstract: We present a *de novo* design of an objective for use in multi-photon (MPM) and second harmonic generation (SHG) microscopy. This objective was designed to have a large field of view (FOV), while maintaining a moderate numerical aperture (NA) and relative straight forward construction. A dichroic beam splitter was incorporated within the objective itself allowing for an increase in the front aperture of the objective and corresponding enhancement of the solid angle of collected emission by an order of magnitude over existing designs.

OCIS codes: (110.2970) Image detection systems; (170.0110) Medical optics and biotechnology: Imaging systems; (170.2520); Medical optics and biotechnology: Fluorescence microscopy; (170.3880) Medical optics and biotechnology: Medical and biological imaging; (180.4315) Nonlinear microscopy; (180.5810) Scanning microscopy; (180.6900) Three-dimensional microscopy; (190.4180) Multiphoton processes; (290.1350) Backscattering

References and links

1. W. Denk, J. H. Strickler, and W. W. Webb, "Two-photon laser scanning fluorescence microscopy," Science **248**(4951), 73–76 (1990).
2. W. R. Zipfel, R. M. Williams, and W. W. Webb, "Nonlinear magic: multiphoton microscopy in the biosciences," Nat. Biotechnol. **21**(11), 1369–1377 (2003).
3. P. Theer, and W. Denk, "On the fundamental imaging-depth limit in two-photon microscopy," J. Opt. Soc. Am. A **23**(12), 3139–3149 (2006).
4. C. A. Combs, A. V. Smirnov, J. D. Riley, A. H. Gandjbakhche, J. R. Knutson, and R. S. Balaban, "Optimization of multiphoton excitation microscopy by total emission detection using a parabolic light reflector," J. Microsc. **228**(Pt 3), 330–337 (2007).
5. J. D. McMullen, and W. Zipfel, "A Scheme for Increasing the Collection Efficiency of Multiphoton Microscopy," Biophys. J. **96**(3), 639a (2009).
6. C. J. Engelbrecht, W. Göbel, and F. Helmchen, "Enhanced fluorescence signal in nonlinear microscopy through supplementary fiber-optic light collection," Opt. Express **17**(8), 6421–6435 (2009).
7. D. Vucinić, T. M. Bartol, Jr., and T. J. Sejnowski, "Hybrid reflecting objectives for functional multiphoton microscopy in turbid media," Opt. Lett. **31**(16), 2447–2449 (2006).
8. M. Lelek, E. Suran, F. Louradour, A. Barthelemy, B. Viellerobe, and F. Lacombe, "Coherent femtosecond pulse shaping for the optimization of a non-linear micro-endoscope," Opt. Express **15**(16), 10154–10162 (2007).
9. W. Göbel, J. N. D. Kerr, A. Nimmerjahn, and F. Helmchen, "Miniaturized two-photon microscope based on a flexible coherent fiber bundle and a gradient-index lens objective," Opt. Lett. **29**(21), 2521–2523 (2004).
10. L. Fu, X. Gan, and M. Gu, "Nonlinear optical microscopy based on double-clad photonic crystal fibers," Opt. Express **13**(14), 5528–5534 (2005).
11. W. R. Zipfel, R. M. Williams, R. Christie, A. Y. Nikitin, B. T. Hyman, and W. W. Webb, "Live tissue intrinsic emission microscopy using multiphoton-excited native fluorescence and second harmonic generation," Proc. Natl. Acad. Sci. U.S.A. **100**(12), 7075–7080 (2003).
12. J. N. Rogart, J. Nagata, C. S. Loeser, R. D. Roorda, H. Aslanian, M. E. Robert, W. R. Zipfel, and M. H. Nathanson, "Multiphoton imaging can be used for microscopic examination of intact human gastrointestinal mucosa ex vivo," Clin. Gastroenterol. Hepatol. **6**(1), 95–101 (2008).
13. S. Mukherjee, J. S. Wysock, C. K. Ng, M. Akhtar, S. Perner, M. M. Lee, M. A. Rubin, F. R. Maxfield, W. W. Webb, and D. S. Scherr, "Human bladder cancer diagnosis using Multiphoton Microscopy," Proc. SPIE **7161**, 1–10 (2009).

#121772 - $15.00 USD Received 18 Dec 2009; revised 22 Jan 2010; accepted 1 Feb 2010; published 1 Mar 2010

14. Y. Shimizu, and H. Takenaka, "Microscope Objective Design," Adv. Opt. Electron Microsc. **14**, 249–334 (1994).
15. W. J. Smith, "Modern Optical Engineering", (McGraw Hill, 2000) Chapter 13.
16. H. Kazuhiro, Olympus Optical Company, Ltd., "Microscope Objective" Japanese Patent 11–231224 (1999)
17. W. F. Cheong, S. A. Prahl, and A. J. Welch, "A Review of the Optical Properties of Biological Tissues," IEEE J. Quantum Electron. **26**(12), 2166–2185 (1990).
18. E. Beaurepaire, and J. Mertz, "Epifluorescence collection in two-photon microscopy," Appl. Opt. **41**(25), 5376–5382 (2002).

1. Introduction

Multiphoton microscopy [1, 2] has developed into a standard tool for the life scientist with far reaching applications ranging from basic cell biology to imaging physiology and disease progression in live animals. This robust form of laser scanning microcopy is ideal for experiments in which cellular and sub-cellular resolution fluorescence imaging is required in a highly scattering medium. As the technique has advanced there has been a corresponding development of new objective lenses specifically for use in multiphoton microscopy. These new designs have increased IR transmission and obtained high numerical apertures (NA) at relatively low magnification (e.g. Olympus 25x/1.05 NA, Zeiss 20x/1.0 NA). Other collection schemes, which exploit the principle that all of the collected emission light in MPM – even the scattered photons – contribute to useable signal [3], have increased the overall solid angle sampled by implementing additional collection optics such as a parabolic reflector underneath the tissue [4], or a ring of waveguides surrounding it [5, 6]. High NA reflecting objectives have also been designed and demonstrated to efficiently collect fluorescence [7].

Although high numerical aperture is important to achieve the highest resolution, there are cases in which the experimenter is willing to sacrifice resolution for an increase in the field of view (FOV), for example in cell tracking experiments in tissues, or for observations of calcium oscillations in a large neuronal networks. Additionally, a wider field of view would be particularly useful for "multiphoton pathology" applications. The translation of MPM from the laboratory to the operating room is currently underway with various research groups developing the first generation of MPM endoscopes [8–10] in the hopes of soon being able to perform *in vivo* optical biopsies. The direct MPM imaging of fresh unstained biopsy tissue has been demonstrated [11–13] to provide instant histological grade images without the tedious preparation necessary to produce standard sectioned slides, and one day may become an indispensable part of clinical practice. In addition, the intrinsic contrast provided both by autofluorescence from endogenous fluorophores such as NADH, flavins and other autofluors, as well as second harmonic generation from such macromolecules as collagen, adds information beyond morphometric parameters. However, some of these signals are weaker than typical dyes by several orders of magnitude [11], and it is therefore critically important to maximize the collection optics for this particular application.

As existing technology has been focused on higher numerical aperture objective designs with fields of view under a millimeter, we decided to develop a new objective design motivated by the following requirements: (1) large field of view; (2) long working distance; (3) a sufficient numerical aperture for reasonable optical sectioning and single cell resolution; (4) collection of as large of a solid angle as possible; (5) an inexpensive design to fabricate; and (6) chromatic correction over at least the bandwidth of a typical femtosecond pulse (10-15 nm).

Based our own large field of view multiphoton imaging needs, we determined that the objective should have a FOV of at least 4 mm at zoom 1 on our scanning microscopes. In addition, the working distance needs to be at least 2 mm. Although that is more than twice the imaging penetration depth of an MPM system, a larger working distance becomes necessary when imaging the irregular surfaces common in tissue and live animal imaging cases. Again based on the needs of typical large FOV imaging experiments, we imposed the requirement that the axial FWHM of the two-photon focal volume be no more than 10 microns maximum,

#121772 - $15.00 USD Received 18 Dec 2009; revised 22 Jan 2010; accepted 1 Feb 2010; published 1 Mar 2010

roughly the thickness of a cell layer. For an objective lens of a NA < 0.7, in an immersion medium of refractive index n, the dimensions (and so the sectioning capability) of the two-photon focal volume can be given as [2]:

$$\omega_{x,y} = \frac{0.32\lambda}{\sqrt{2}NA} \qquad \omega_z = \frac{0.532\lambda}{\sqrt{2}}\left[\frac{1}{n-\sqrt{n^2-NA^2}}\right] \tag{1}$$

where $\omega_{x,y}$ and ω_z are the lateral and axial 1/e waist of the focal volume for a given wavelength λ. Using these equations we determined that our minimum resolution specification was met by an NA of ~0.3 in air and ~0.35 for an objective designed to be immersed in water. The upper limit on objective NA is also set by the size of the lens back aperture. To achieve the optical resolution possible by a given lens numerical aperture, the 1/e diameter of the laser beam at the objective back aperture must on the order the diameter of the entrance pupil. We set a design threshold of no more than 25 mm for the diameter of this stop, which we can accommodate in our scanning systems using a scan lens/tube lens combination that produces a ~12x increase in the laser beam diameter to provide a nearly overfilled back aperture. Although this reduces our scan angle, this lens design achieves a large FOV at relatively small field angles.

To maximize the objective's ability to collect emissions, we increased the acceptance solid angle by enlarging the diameter of the front aperture. An infinity corrected fluorescence objective is designed to collimate light originating from its focal plane so that that it can be translated onto a distant image plane and, as a result, the diameter of its front aperture is dictated by its working distance and NA. However, by incorporating a dichroic element into the objective itself, the need to collimate this light in order to send it to a distant detector can be relaxed. This allows for an increase in the size of the front aperture of the objective as well as the application of a reflective coating to the interior of the objective casing, both of which boost the collected solid angle far in excess of what one would predict based on NA alone. Our design effectively decouples the excitation and emission paths within the objective lens.

Throughout the design process an effort was made to limit the fabrication cost of the system. The number of lens elements was kept as low as possible – 3 for the air objective with the addition of one additional meniscus lens element to compensate for aberration when water was used as an immersion medium [14]. No aspheric surfaces were used, though they could be implemented to further increase the field of view of the system or the NA. All glasses are stock and were selected to minimize fabrication cost. Only two glass types were used in the two designs (Schott SF2 and Schott NSK16 – see Table 1).

The objective lens was designed to deliver excitation light centered at 780 nm with all of the optics having a default ¼ wavelength magnesium fluoride coating. The system was designed to support a bandwidth of greater than 10 nm (775, 780, and 785 nm all being equally weighted during calculations). Although the reference wavelength was 780 nm, the objective performed well throughout the range of the Ti:Sapphire laser, with only a small relative shift in the focal plane occurring for different excitation wavelengths (e.g. ~35 μm at 880 nm). Although dispersion due to the focusing elements and beam splitter might appear to be problem at first glance, this design is not substantially more dispersive material than other lenses of similar NA and FOV [16] based on total glass thickness. With the current trend of pre-compensation systems being incorporated into commercial Ti:Sapphire lasers (e.g. Spectra Physics DeepSee) it should be possible to deliver transform limited pulses through it.

2. Design

The ray tracing software Code V (Optics Research Associates, Optics Research Associates, Pasadena, CA) was used to design both an air and a water immersion version of the lens (Fig. 1 and Table 1) whose properties are summarized below (Table 2). The air immersion lens had an NA of 0.3 and a full FOV of 4 mm from an input field angle of ±2.8°. The water objective

#121772 - $15.00 USD Received 18 Dec 2009; revised 22 Jan 2010; accepted 1 Feb 2010; published 1 Mar 2010

requires a beam tilt of ±3.5° to cover its full field of view, but the higher index of refraction of water increases the numerical aperture to 0.35 and slightly decreases the diameter of the back aperture. Both lenses have a working distance of 2 mm. An emission-splitting plate dichroic placed directly after the front lens was found to severely degrade the point spread function, however a dichroic coated beam splitting cylindrical wedge incorporated into the lens design at that point produced no significant degradation after optimization [15]. The emission diverting optic is large, matching of the typical diameter of a photomultiplier tube (PMT) photocathode (~20 mm). However, the rays at this point could also be efficiently coupled into a high NA, high transmission light guide for example to direct to a more distant multichannel detection system.

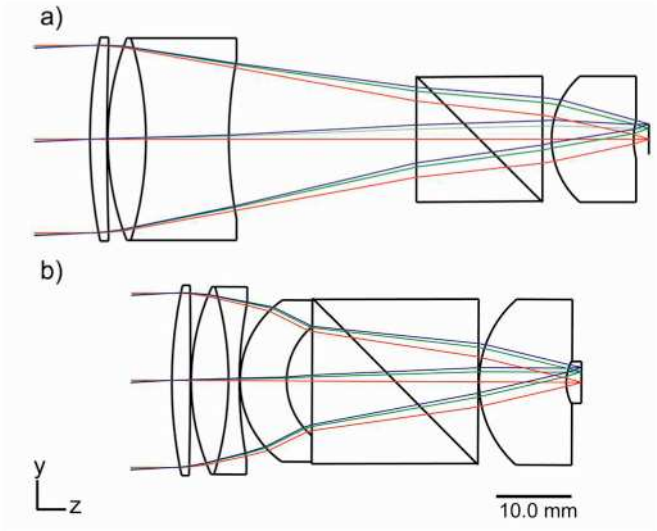

Fig. 1. The design of an objective incorporating a beam splitter to efficiently decouple the excitation and collection path (a) air immersion, (b) water immersion

The performance of the lens is close to the diffraction limit. The composite Strehl ratio (Table 2), consisting of all three equally weighted wavelengths, meets the *Marechal* criterion for each lens for all three calculated angles, indicating effectively diffraction limited performance across the field. This is confirmed by the modulation transfer functions (MTF) (Fig. 2 a,d) for both designs where the tangential and radial components of each field approximate the diffraction limited curve. The MTF shown in Fig. 2 was calculated based on the single photon PSF; the MTF is further improved using two-photon excitation and the two-photon PSFs at the extreme of the field of view (Fig. 2 b,e) were found to be effectively diffraction limited. Small amounts of aberration (mainly coma) in the single photon point spread function are minimized by the squaring of the PSF. Finally, the field curvature for both the lenses (Fig. 2 c,f) was calculated and found to be within the axial FWHM, with fairly good overlap between the tangential and sagittal rays indicating minimal astigmatism.

#121772 - $15.00 USD Received 18 Dec 2009; revised 22 Jan 2010; accepted 1 Feb 2010; published 1 Mar 2010

Table 1. Surface Properties of the Air and Water Immersion Objectives

Air Immersion				Water Immersion			
Surface #	**Y Radius (mm)**	**Thickness (mm)**	**Glass**	**Surface #**	**Y Radius (mm)**	**Thickness (mm)**	**Glass**
1	68.2985	2.2476	NSK16	1	58.9079	2.4530	NSK16
2	388.6545	0.1000		2	–679.5758	0.1000	
3	37.0318	5.0358	NSK16	3	30.0456	4.9294	NSK16
4	–45.7979	10.9444	SF2	4	–42.4262	1.4364	SF2
5	54.7121	24.7277		5	55.0440	0.1000	
6	∞	8.3230	SF2	6	13.0909	6.1429	NSK16
7	∞	8.3230	SF2	7	9.4734	3.3587	
8	∞	1.2197		8	∞	10.9560	SF2
9	11.1877	10.8314	NSK16	9	∞	10.9560	SF2
10	9.8498	2.0000		10	∞	0.1000	
Image	∞			11	14.6654	11.5217	SF2
				12	6.0563	2.0000	WATER
				Image	∞	0	

Table 2. A Summary of Objective Lens Parameters

	Entrance pupil (mm)	NA	Field Angle (°)	Focus Position (mm)	Strehl Ratio
Air Lens	24.8	0.3	0	0	0.963
			2	1.43	0.971
			2.8	2	0.869
Water Lens	23.1	0.35	0	0	0.885
			2.5	1.43	0.868
			3.5	2	0.812

3. Analysis

To assess the overall collection efficiency of our lens design we conducted Monte Carlo simulations using the non-sequential ray tracer LightTools (v6.3 Optics Research Associates, Pasadena, CA). This allowed us to calculate the overall "collection numerical aperture" of our lenses which was different than numerical aperture of the excitation focusing pathway. We compared these designs to the Olympus 4x XLFLUOR, a commercially available macro objective with an NA of 0.28 – approximately 1.75x the typical NA of a standard 4x. This macro lens has been our primary objective lens for large FOV multiphoton imaging in our lab. The lens model we used for our comparison was based on the design shown in the Olympus patent [16] and had a slightly smaller NA (0.27) and working distance (28.1 mm) compared to the commercially available Olympus 4x macro objective (NA=0.28 and WD=29.5 mm). Another minor difference in the design shown in the patent was that it was corrected for a sample immersed in 6 mm of water rather than the 5 mm water layer the commercially available 4x objective is designed around. The three objective lens designs (our air and water designs, and the Olympus 4x) were imported from Code V into LightTools (Fig. 3) and an enclosure was placed around the system with an opening for the detector (receiver surface – Fig. 3a) which was placed perpendicular to the optical axis (only one detector was considered for simplicity). In order to collect as many photons as possible, the inner side of the objective

#121772 - $15.00 USD Received 18 Dec 2009; revised 22 Jan 2010; accepted 1 Feb 2010; published 1 Mar 2010

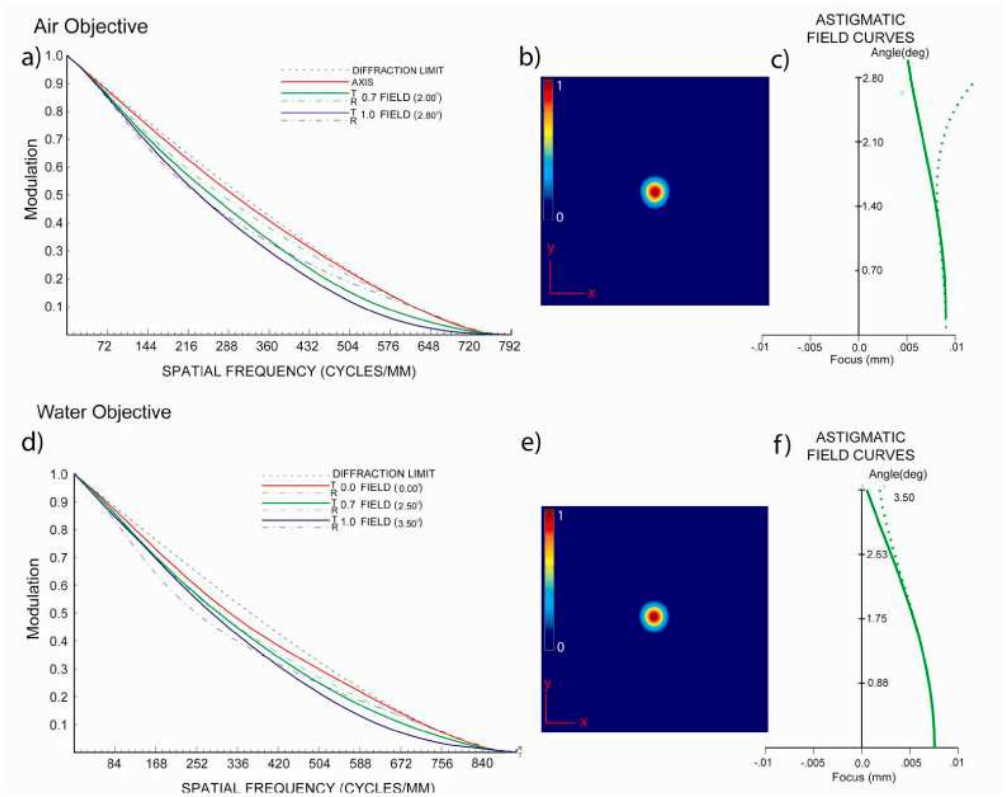

Fig. 2. Characterization of the excitation transmission for the air and water immersion objectives (a,d) modulation transfer function (b,e) two photon PSF at the greatest field angle - scale bar = 2μm (c,f) field curvature at the edge of the field for the tangential (dashed) and sagittal (solid) surfaces.

enclosure was set to be reflective at and below the beam splitter (Fig. 3d) and the lateral edges of the optical components were assumed to be transmitting. In the Olympus objective simulation a 50.8 mm square dichroic mirror was placed 10 cm along the optical axis away from the back aperture. This was focused into a receiver of 20 mm diameter (the size of our PMT photocathode) by a lens 40 mm wide. This simulation layout is similar to our current large FOV multiphoton imaging systems and represents a typical optimal setup on a standard microscope frame where the focusing nosepiece and other frame parts dictate a ~10 cm minimum spacing. The coatings on both the internal dichroic (our lens models) and the external dichroic (4x objective model) were modeled as 100% reflective. In order to assess the effective collection NA (NA_c) of the objectives in their respective immersion media (without any scattering), we first examined the collected fraction of photons from an isotropically radiating 587 nm point source located at the intersection of the optical axis and the focal plane. By equating this to the fraction of total solid angle, it is possible to derive the equation for the numerical aperture of collection:

$$NA_c = n\sin\left(\cos^{-1}(1-2\Phi)\right) \tag{2}$$

where Φ is the fraction of the total radiated photons that were incident on the detector. The values of NA_c as displayed in Table 3 were found to be greatly enhanced for the new objectives due to the acceptance of the large front aperture and the internal dichroic.

#121772 - $15.00 USD Received 18 Dec 2009; revised 22 Jan 2010; accepted 1 Feb 2010; published 1 Mar 2010

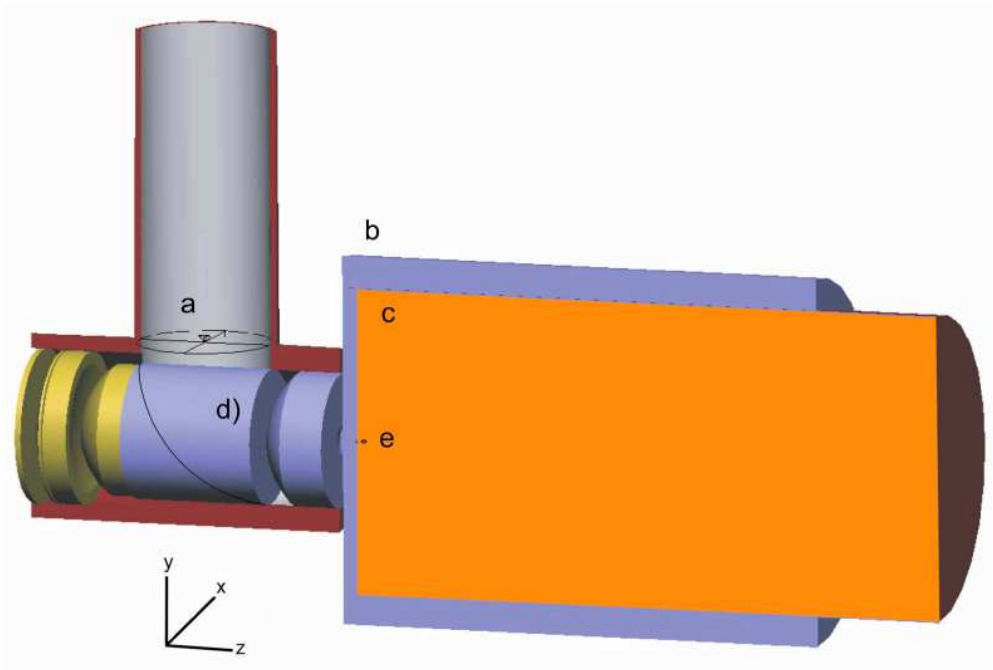

Fig. 3. A cross-section of the water immersion objective modeled using LightTools a) receiver b) water c) tissue slab d) beam splitter e) point source (scale bar ≈1 cm)

Table 3. A Summary of The Lens' Numerical Apertures

Objective	Calculated Numerical Aperture (NA)	Observed Numerical Aperture (NA_c)
Olympus 4x	0.27	0.27
Air Objective	0.30	0.82
Water Objective	0.35	0.98

The objectives were also compared for their ability to collect light from a scattering sample. In this case, a cylindrical tissue slab 50 mm in diameter and 100 mm long (Fig. 3c) was constructed as a volume scatterer using a Mie scattering model at a wavelength of 587 nm. The scattering mean free path and anisotropy factor g for the tissue were set to 0.05 mm and 0.95 respectively, with a bulk refractive index of the material being 1.33. A small amount of absorption at 587 nm was also included in the model, corresponding to a transmittance per unit length of 0.87 – approximating that of human bladder [17]. Light was simulated emitting isotropically from a point source located inside the tissue slab (Fig. 3(e)). The number of photons collected was assessed at various points in the focal plane, as well as at various depths within the tissue. For the two new objectives, 10^5 photons were simulated, each with a maximum of 10^4 allowed scattering events. For the Olympus 4x objective, 10^6 photons were launched to obtain reproducible results, necessitated by the smaller number of rays that reached the detector surface.

The results from these experiments are plotted in Fig. 4(a). Our objective designs collect roughly an order of magnitude more fluorescence than the standard 4x macro lens. It should be noted that the collection of all three objectives was enhanced by scattering from tissue.

#121772 - $15.00 USD Received 18 Dec 2009; revised 22 Jan 2010; accepted 1 Feb 2010; published 1 Mar 2010

This occurs in simulation because the depth of the focus is shallow compared to the length of the "tissue", resulting in the bulk of the tissue acting as a mirror to photons that had initially been radiated away from the lens, but are eventually scattered backwards. This effect is dependent on the particular simulation parameters such as number scattering events allowed, sample absorption and length of the simulated tissue. The magnitude of this effect has been shown [18] to increase with the field of view of the lens.

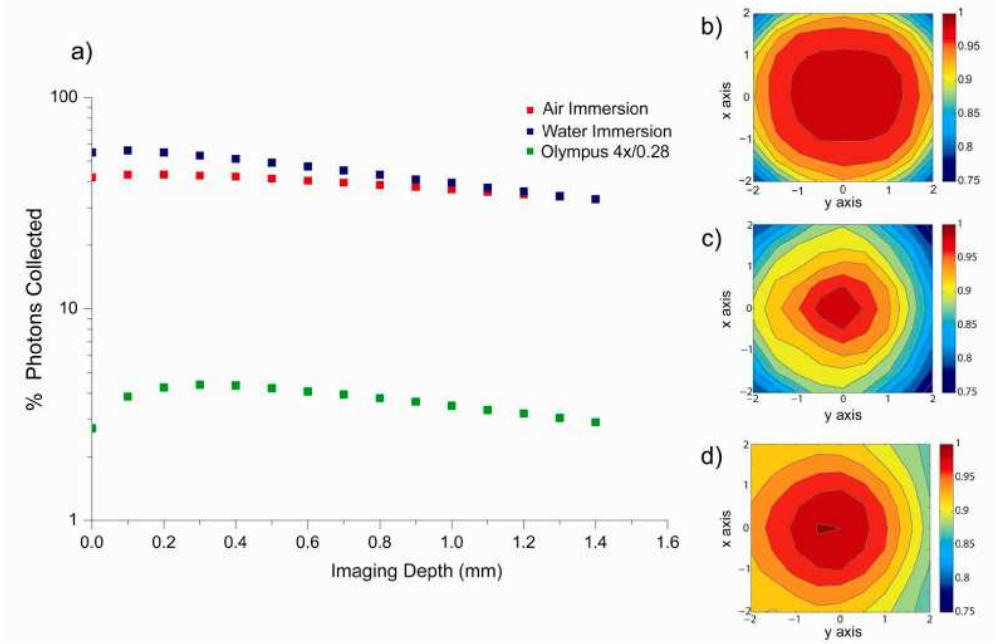

Fig. 4. Simulated light collection in a scattering material. a) Fractional collection as a function of depth of the (on-axis) photon origin in the scattering material. b-d) Spatial variance in the collection path. Collection of scattered light calculated for differing photon origins positions over the FOV relative to the optical axis. b) Olympus 4x objective with focal plane near surface, c) water immersion objective for focal plane near surface, and d) the water immersion objective with the focal plane 500 μm into the simulated tissue.

We examined spatial variance in the collection path by moving the point source about the focal plane at half integer intervals between −2 and +2 mm, and tallying the number of rays reaching the receiver at each point. The number of counts – relative to the center of the field of view – was observed to fall off for all three objective designs, although the value was above 75% of the maximum in all cases. However, unlike the 4x lens (Fig. 4b) which appeared radially symmetric about the optical axis, the incorporation of the dichroic element created a slight asymmetry in the collection path for both the water (Fig. 4c) and air lenses (not shown, but similar to Fig. 4c). Increased scattering appeared to partially curb this effect for the water immersion lens which improved substantially even at moderate depths (Fig. 4d), although both the air immersion variant and the Olympus lens showed no change of this ratio with depth.

4. Summary

We have demonstrated a new design for multiphoton objective lenses specifically for use in cases where large fields of view and high collection efficiencies are required. The objective lens designs presented have a 4 mm large field of view, a moderately low, but useable, focusing NA, with an effective collection NA approaching 1. The designs were demonstrated to be highly efficient at collecting fluorescence, especially in the scattering samples typical of

#121772 - $15.00 USD Received 18 Dec 2009; revised 22 Jan 2010; accepted 1 Feb 2010; published 1 Mar 2010

multiphoton microscopy. The incorporation of such an objective/detector system on an existing microscope should have immediate impact in experiments such as studies of neuronal network signaling, imaging cell migration in tissues explants and live animals, characterization of engineered tissue constructs and promising new areas such as “instant pathology” based on rapid multiphoton imaging of biopsy samples.

Acknowledgments

This work is supported by the National Institutes of Health (NCI R01 CA116583 and NIBIB P41 RR04224 to WRZ). We would like to thank Olympus Inc. for helpful discussions and for providing design information on their 4x macro objective lens, Optical Research Associates for providing Code V and LightTools software packages, and Avtar Singh and Dr. Rebecca Williams for useful discussion and comments.

#121772 - $15.00 USD Received 18 Dec 2009; revised 22 Jan 2010; accepted 1 Feb 2010; published 1 Mar 2010